

Review

# A Review of Sulfate Radical-Based and Singlet Oxygen-Based Advanced Oxidation Technologies: Recent Advances and Prospects

Zhendong Li <sup>1</sup>, Yanmei Sun <sup>2</sup>, Dongfang Liu <sup>3</sup>, Malan Yi <sup>1,\*</sup>, Fang Chang <sup>1</sup>, Huiting Li <sup>1</sup> and Yunyi Du <sup>1</sup>

<sup>1</sup> Research Centre for Coastal and Marine Resource Utilization, Tianjin Research Institute for Water Transport Engineering, Ministry of Transport, Tianjin 300456, China

<sup>2</sup> Construction Management Department, Tianjin Eco-City Water Investment and Construction Co., Ltd., Tianjin 300457, China

<sup>3</sup> Faculty of Environmental Science and Engineering, Nankai University, Tianjin 300350, China

\* Correspondence: yimalan@163.com

**Abstract:** In recent years, advanced oxidation process (AOPs) based on sulfate radical ( $\text{SO}_4^{\bullet-}$ ) and singlet oxygen ( $^1\text{O}_2$ ) has attracted a lot of attention because of its characteristics of rapid reaction, efficient treatment, safety and stability, and easy operation.  $\text{SO}_4^{\bullet-}$  and  $^1\text{O}_2$  mainly comes from the activation reaction of peroxymonosulfate (PMS) or persulfate (PS), which represent the oxidation reactions involving radicals and non-radicals, respectively. The degradation effects of target pollutants will be different due to the type of oxidant, reaction system, activation methods, operating conditions, and other factors. In this paper, according to the characteristics of PMS and PS, the activation methods and mechanisms in these oxidation processes, respectively dominated by  $\text{SO}_4^{\bullet-}$  and  $^1\text{O}_2$ , are systematically introduced. The research progress of PMS and PS activation for the degradation of organic pollutants in recent years is reviewed, and the existing problems and future research directions are pointed out. It is expected to provide ideas for further research and practical application of advanced oxidation processes dominated by  $\text{SO}_4^{\bullet-}$  and  $^1\text{O}_2$ .

**Keywords:** sulfate radical; singlet oxygen; AOPs; peroxymonosulfate; persulfate; decontamination



**Citation:** Li, Z.; Sun, Y.; Liu, D.; Yi, M.; Chang, F.; Li, H.; Du, Y. A Review of Sulfate Radical-Based and Singlet Oxygen-Based Advanced Oxidation Technologies: Recent Advances and Prospects. *Catalysts* **2022**, *12*, 1092. <https://doi.org/10.3390/catal12101092>

Academic Editors: Yuwei Pan, Xiang Li, Yizhen Zhang, Xuedong Du, Jingju Cai, Lu Gan, Qi Zhang and Jun Jiang

Received: 5 September 2022

Accepted: 17 September 2022

Published: 21 September 2022

**Publisher's Note:** MDPI stays neutral with regard to jurisdictional claims in published maps and institutional affiliations.



**Copyright:** © 2022 by the authors. Licensee MDPI, Basel, Switzerland. This article is an open access article distributed under the terms and conditions of the Creative Commons Attribution (CC BY) license (<https://creativecommons.org/licenses/by/4.0/>).

## 1. Introduction

With the development of economy and science and technology, more and more new substances are developed and manufactured to meet the growing needs of human beings. At the same time, many emerging pollutants, such as pesticides, pharmaceuticals and personal care products (PPCPs), polycyclic aromatic hydrocarbons (PAHs), perfluorinated compounds (PFCs), food additives, surfactants, plasticizers, and pathogens, are released into the aquatic environment during production, processing, use, and waste. As these pollutants migrate and transform in the environment, they accumulate in organisms and eventually harm human health. These emerging pollutants have relatively stable properties, complex molecular structures and are difficult to degrade in the natural environment, so they cannot be completely degraded by traditional biological processes [1,2].

In recent decades, water treatment technologies have achieved rapid development. Especially, advanced oxidation processes (AOPs) have been applied to the degradation, complete mineralization or pretreatment of complex and refractory organic pollutants. Compared with traditional water treatment methods, advanced oxidation technology has obvious advantages of strong oxidation capacity, fast reaction rate, simple operation, wide application range, high treatment efficiency, less secondary pollution, high mineralization rate, equipment, and large-scale application. AOPs relies on reactive oxygen species (ROS) to degrade organic pollutants. Among them, sulfate radical ( $\text{SO}_4^{\bullet-}$ ) and singlet oxygen ( $^1\text{O}_2$ ) have attracted more and more researchers' attention due to their unique properties in

the removal of organic pollutants [3,4]. Compared with the traditional hydroxyl radical ( $\bullet\text{OH}$ ),  $\text{SO}_4^{\bullet-}$  has a higher redox potential (2.5–3.1 V), and the redox potential of  $\bullet\text{OH}$  is 2.7 V and 1.8 V under acidic and alkaline conditions, respectively. In addition,  $\text{SO}_4^{\bullet-}$  (30–40  $\mu\text{s}$ ) has a longer half-life than  $\bullet\text{OH}$  (20 ns) [5].  $\text{SO}_4^{\bullet-}$  also degrades many organic compounds more efficiently than  $\bullet\text{OH}$ , due to its greater selectivity for electron transfer reactions, giving  $\text{SO}_4^{\bullet-}$  a greater advantage in mineralizing a wide range of organic pollutants [6]. Moreover, the oxidation efficiency of  $\text{SO}_4^{\bullet-}$  in carbonate and phosphate buffer solutions is higher than that of  $\bullet\text{OH}$  [7]. Therefore, sulfate radical-based AOPs will have better oxidation efficiency and application than hydroxyl radical-based AOPs.

Unlike  $\text{SO}_4^{\bullet-}$  and  $\bullet\text{OH}$ ,  $^1\text{O}_2$  is a non-free radical ROS, which can degrade organic pollutants through non-free radical attack pathways [8].  $^1\text{O}_2$  is electrophilic and highly selective for electron-rich organic matter, which facilitates selective removal of micropollutants (e.g., drugs and endocrine disruptors) in the presence of salinity and other organic matter [9,10]. Therefore, the non-radical oxidation reaction based on  $^1\text{O}_2$  provides an idea for the removal of refractory organic compounds in complex matrix.

$\text{SO}_4^{\bullet-}$ -based and  $^1\text{O}_2$ -based AOPs have attracted increasing interest. Most of the recent studies focus on the generation of  $\text{SO}_4^{\bullet-}$  and  $^1\text{O}_2$  and the degradation of one or several organic pollutants. However, there are few reports on the comprehensive evaluation of the formation, mechanism, and application of  $\text{SO}_4^{\bullet-}$  and  $^1\text{O}_2$ . This paper reviews the recent progress and prospect about sulfate radicals-based and singlet oxygen-based advanced oxidation technologies. The production of  $\text{SO}_4^{\bullet-}$  and  $^1\text{O}_2$  mainly comes from the activation of persulfate (PS) and peroxymonosulfate (PMS). The chemical properties of PMS and PS are briefly introduced in this paper, and the generation, reaction mechanism, and treatment effect of  $\text{SO}_4^{\bullet-}$ -based and  $^1\text{O}_2$ -based AOPs are emphasized. The obstacles in the current research work are pointed out and the future research is prospected. It is expected to provide ideas for further research and practical application of AOPs based on  $\text{SO}_4^{\bullet-}$  and  $^1\text{O}_2$ . This paper has a certain reference and guiding significance for the applications of PMS or PS activation technologies in environmental pollution control and remediation.

## 2. Characteristics of Persulfate and Peroxymonosulfate

At present, the production of  $\text{SO}_4^{\bullet-}$  mainly comes from the activation of PMS and PS, which are the monosubstituted or symmetrically substituted derivatives of hydrogen peroxide by sulfonic acid group ( $-\text{SO}_3$ ), respectively. PMS has been widely used in organic compound synthesis and as a chlorine-free additive for disinfecting swimming pools at a rate of about 1–2 pounds per 10,000 gallons of pool water [11]. Under the presence of 25 mg/L PMS and 0.1 mg/L  $\text{Co}^{2+}$ , the removal rate of *E. coli* reached 99.99% after 1 h of reaction [12]. PMS is white solid powder. It is stable when pH is less than 6 or pH is 12. When pH is 9, it showed the poorest stability where half of  $\text{HSO}_5^-$  decomposes to  $\text{SO}_5^{2-}$  [4]. At present, the widely used potassium bisulfate complex salt ( $2\text{KHSO}_5 \cdot \text{KHSO}_4 \cdot \text{K}_2\text{SO}_4$ ) is composed of three components, potassium peroxymonosulfate, potassium hydrogen sulfate, and potassium sulphate, and its main active substance is potassium peroxymonosulfate ( $\text{KHSO}_5$ ). The salt is marketed under the trade names Caroat and Oxone registered by Evonik and DuPont, respectively. Oxone is a white granular powder crystal salt, which is stable, non-toxic, inexpensive, and soluble in water. The peroxide bond (O-O) distance is 1.453 Å, and the bond energy is 140–213.3 kJ/mol. PMS is most stable when the solution pH is less than 6 and equal to 12. When pH is 9, the stability is worst, and the concentration of  $\text{HSO}_5^-$  and  $\text{SO}_5^{2-}$  in the solution is almost equal. When pH is less than 1, PMS will undergo hydrolysis reaction to produce  $\text{H}_2\text{O}_2$  [13]. PS, an oxidant with symmetrical structure, was first known as the initiator of polymerization reaction. The O-O distance is 1.497 Å, and the bond energy is 140 kJ/mol [14]. PS, often in the form of potassium persulfate or sodium persulfate, has been widely used as bleaching agents, oxidants, emulsion polymerization promoters, and water or soil remediation agents. The related properties of PMS and PS are shown in Table 1. Both PMS and PS are strong oxidants, but their direct reaction rates

with most pollutants are very low. Therefore, it is necessary to activate them through appropriate ways to destroy the O-O bond and generate strong oxidizing free radicals,  $^1\text{O}_2$  and other ROS to degrade organic pollutants quickly and efficiently.

**Table 1.** Properties of PMS and PS.

Properties	PS (Take Potassium Persulfate as an Example)	PMS (Take Potassium Peroxymonosulfate as an Example)
CAS Registry Number	7727-21-1	10058-23-8
Chemical formula	$\text{K}_2\text{S}_2\text{O}_8$	$\text{KHSO}_5$
Molecular mass	270.309	614.738
Solubility in water (20 °C)	520 g/L	>250 g/L
Redox potential	2.01 V	1.82 V

Because PS and PMS are solid powders, they can be transported and stored more easily. Compared with  $\text{H}_2\text{O}_2$ , the anions of PS and PMS remain stable in water for a much longer time until they are properly activated. In addition, PMS and PS-based AOPs can proceed smoothly in a wide solution pH range from acidic to alkaline (pH = 2–10), while  $\text{H}_2\text{O}_2$ -based Fenton process requires strict acidic conditions (pH = 2.7–3). Generally, PS and PMS can be activated with the assistance of ultraviolet light, heat, alkali, or metal catalysts, etc. Different types of oxidants and activation methods will produce different ROS. The advanced oxidation processes dominated by  $\text{SO}_4^{\bullet-}$  and  $^1\text{O}_2$  were discussed in this paper.

### 3. Sulfate Radicals-Based Advanced Oxidation

Studies have shown that AOPs based on  $\text{SO}_4^{\bullet-}$  and  $\bullet\text{OH}$  is an effective method for the degradation of refractory organic pollutants, such as pharmaceuticals, pesticides, personal care products, steroids, endocrine disruptors, etc. [15]. However, AOPs based on  $\bullet\text{OH}$  degrades organic pollutants through a non-selective, multi-step approach that typically requires an acidic environment. In addition, the oxidation process is severely limited by the large amount of dissolved organic matter and anions in complex environments, which are the main scavengers of  $\bullet\text{OH}$ .  $\text{SO}_4^{\bullet-}$  is inherently more oxidizing than  $\bullet\text{OH}$  and lasts longer in aqueous solutions, and in some cases  $\text{SO}_4^{\bullet-}$  can oxidize contaminants that  $\bullet\text{OH}$  cannot. In recent years,  $\text{SO}_4^{\bullet-}$ -based AOPs have replaced  $\bullet\text{OH}$ -based AOPs to some extent.

The essence of the advanced oxidation process based on  $\text{SO}_4^{\bullet-}$  is to activate PMS or PS to form  $\text{SO}_4^{\bullet-}$  to achieve the removal of organic matter. Besides  $\text{SO}_4^{\bullet-}$ , there are also associated or indirect generation of  $\bullet\text{OH}$ , superoxide radical ( $\text{O}_2^{\bullet-}$ ), or other radicals, but  $\text{SO}_4^{\bullet-}$  plays a leading role in the degradation of pollutants. These free radicals ( $\text{SO}_4^{\bullet-}$ ,  $\bullet\text{OH}$ , and  $\text{O}_2^{\bullet-}$ ) could be detected by using 5,5-dimethyl-1-pyrroline-1-oxide (DMPO) as a spin trapping agent in an electron paramagnetic resonance spectroscopy (EPR) [16]. Both ethanol (Et) and tert-butanol (TBA) could quench  $\bullet\text{OH}$  rapidly ( $k_{\text{Et}} = 1.2\text{--}2.8 \times 10^9 \text{ M}^{-1}\text{s}^{-1}$ ,  $k_{\text{TBA}} = 3.8\text{--}7.6 \times 10^8 \text{ M}^{-1}\text{s}^{-1}$ ), and the reaction rate between Et and  $\text{SO}_4^{\bullet-}$  is much faster than that of TBA ( $k_{\text{Et}} = 1.6\text{--}7.7 \times 10^7 \text{ M}^{-1}\text{s}^{-1}$ ,  $k_{\text{TBA}} = 4.0\text{--}9.1 \times 10^5 \text{ M}^{-1}\text{s}^{-1}$ ). Therefore, Et and TBA can be used as capture agents to identify who contributes more to the degradation of pollutants [17]. PMS and PS can be activated to produce  $\text{SO}_4^{\bullet-}$  through energy input, transition metal ions and their oxides, non-metallic materials, etc. Studies on the degradation of pollutants by activating PMS and PS in different ways to generate  $\text{SO}_4^{\bullet-}$  are summarized in Table 2.

**Table 2.** PMS and PS radical activation with various method for the removal of pollutants.

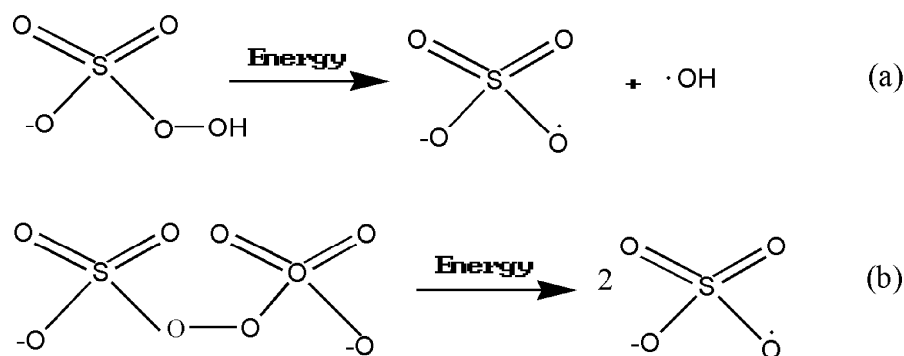
Reaction System	Pollutant	Conditions	Reactivity	Dominant ROS	Ref.
UV(254 nm)/PMS	benzoic acid (BA)	[BA] = 9.90 $\mu$ M; [PMS] = 100 $\mu$ M as 1/2 Oxone; pH = 11.	>90% with 10 min	SO <sub>4</sub> <sup>•-</sup> and •OH	[18]
UV(254 nm)/PS	Chlorophene	[Chlorophene] = 1 $\mu$ M, [PS] = 50 $\mu$ M, pH = 7, UV intensity (254 nm,15 W) = 4.23 mWcm <sup>-2</sup> .	100% with 5 min	SO <sub>4</sub> <sup>•-</sup>	[19]
UV-C laser/PS	Iohexol (IOX)	I <sub>UV</sub> = 25 mW/cm <sup>2</sup> , [PS] = 1.0 mM, [IOX] = 10 $\mu$ M, initial pH = 7.0 $\pm$ 0.5, temperature 25 °C.	93.8% within only 40 s	SO <sub>4</sub> <sup>•-</sup>	[20]
Heat/PS	Ibuprofen (IBU)	[phosphate buffer] = 0.09 M, pH = 7.0, [IBU] = 20.36 $\mu$ M, [PS] = 1.0 mM, T = 70 °C.	100% with 20 min	SO <sub>4</sub> <sup>•-</sup> and •OH	[21]
Heat/PS	1-alkyl-3-methylimidazolium bromides (C <sub>4</sub> mimBr)	[C <sub>4</sub> mimBr] = 0.1 mM, [PS] = 10 mM, T = 60 °C, pH = 7, V = 100 mL.	100% with 120 min	SO <sub>4</sub> <sup>•-</sup>	[22]
Ultrasound/PS	1,1,1-trichloroethane (TCA)	[TCA] = 25.0 mg/L, [PS] = 250.0 mg/L pH 7.0, T = 20 $\pm$ 2 °C, ultrasound: 400 kHz, 100 W.	100% with 120 min	SO <sub>4</sub> <sup>•-</sup>	[23]
Electrolysis(boron-doped diamond anode)/PS	Ampicillin	[Ampicillin] = 1.1 mg/L, [PS] = 250 mg/L, current density (BDD anode) = 25 mAcm <sup>-2</sup> .	100% with 120 min	SO <sub>4</sub> <sup>•-</sup> and •OH	[24]
Fe <sup>0</sup> /PS	sulfamethoxazole (SMX)	[SMX] = 39.5 $\mu$ M, [PS] = 1.0 mM, [Fe <sup>0</sup> ] = 2.23 mM; m (Fe <sup>0</sup> ) = 2.5 mg, pH = 3.52.	100% with 30 min	SO <sub>4</sub> <sup>•-</sup>	[25]
Fe <sup>2+</sup> /PS	Acetaminophen (ACT)	[ACT] = 0.05 mM, [Fe <sup>2+</sup> ] = 1 mM, [PS] = 0.8 mM, pH = 3, T = 20 °C.	70% with 30 min	SO <sub>4</sub> <sup>•-</sup>	[26]
Fe(II)/PMS	2-chlorobiphenyl (2-CB)	[2-CB] = 0.0212 mM; [Fe(II)] = 0.11 mM; [PMS] <sub>0</sub> = 0.11 mM.	90% with 240 min	SO <sub>4</sub> <sup>•-</sup>	[27]
Co <sup>2+</sup> /PMS	nuclear grade cationic IRN-77 resin	initial pH = 9, [Co <sup>2+</sup> ] = 4 mM, [PMS] = 60 mM T = 60 °C.	~90% COD removal (1000 mg/L) with 60 min	SO <sub>4</sub> <sup>•-</sup> and •OH	[28]
Cu <sup>2+</sup> /PMS	Triclosan (TCS)	[TCS] = 9 mg/L (0.031 mM), initial pH = 7, molar ratio of oxidant to metal = 1:1, molar ratio of oxidant to triclosan = 5:1.	95% with 10 min	SO <sub>4</sub> <sup>•-</sup>	[29]
Ru <sup>3+</sup> /PMS	2,4-dichlorophenol (2,4-DCP)	[2,4-DCP] = 0.311 mM, [RuCl <sub>3</sub> ·xH <sub>2</sub> O] = 2.553 mM, [KHSO <sub>5</sub> ] = 1.244 mM, pH = 7.	98% in less than 1 min	SO <sub>4</sub> <sup>•-</sup>	[30]
Natural chalcopyrite/PMS	Bisphenol S	Bisphenol S = 25 $\mu$ M, chalcopyrite = 2 g/L, PMS = 0.4 mM, initial pH = 6.2, T = 303 K.	83% with 30 min	SO <sub>4</sub> <sup>•-</sup> and •OH	[31]
Eggshell-loaded CoFe <sub>2</sub> O <sub>4</sub> /PMS	Florfenicol (FF)	CoFe <sub>2</sub> O <sub>4</sub> /eggshell = 0.4 g/L, [PMS] = 0.96 mmol/L, [FF] = 10 mg/L, T = 30 °C, initial pH = 6.61.	96.8% within 40 min	SO <sub>4</sub> <sup>•-</sup> and •OH	[32]

Table 2. Cont.

Reaction System	Pollutant	Conditions	Reactivity	Dominant ROS	Ref.
CoFe layered double oxide/g-C <sub>3</sub> N <sub>4</sub> /PMS	paracetamol	[catalyst] = 0.2 g/L, [PMS] = 0.5 mM, [paracetamol] = 10 mg/L, temperature = 25 ± 0.5 °C, initial pH = 7 ± 0.2.	100% in less than 10 min	SO <sub>4</sub> <sup>•−</sup>	[33]
Co <sub>3</sub> O <sub>4</sub> /PMS	Acid Orange 7	[AO7] = 0.2 mM, [PMS] = 2 mM and [nano-Co <sub>3</sub> O <sub>4</sub> ] = 0.5 g/L, pH = 7.	100% with 60 min	SO <sub>4</sub> <sup>•−</sup>	[34]
Co-MCM41	Caffeine (CAF)	[CAF] = 0.05 mM, [PMS] = 0.2 mM, [catalyst] = 200 mg/L, pH = 7.10.	100% with 15 min	SO <sub>4</sub> <sup>•−</sup> and •OH	[35]
Ag <sub>0.4</sub> -BiFeO <sub>3</sub> /PS	tetracycline (TC)	[catalysts] = 300 mg/L, [PS] = 5 mM, [TC] = 10 mg/L, pH = 4.5, T = 298 K.	91% with 60 min	SO <sub>4</sub> <sup>•−</sup> and •OH	[36]
S-doped α-Fe <sub>2</sub> O <sub>3</sub> /PS	carbamazepine (CBZ)	[CBZ] = 2 mg/L, [PS] <sub>0</sub> = 0.2 mM, [catalyst] = 0.2 g/L, T = 25 ± 1 °C and initial pH = 6.8 ± 0.5.	93.13% with 30 min	SO <sub>4</sub> <sup>•−</sup>	[37]
Fe <sub>3</sub> O <sub>4</sub> @Zn/Co-ZIFs/PMS	carbamazepine (CBZ)	[CBZ] = 5 mg/L, [catalyst] = 25 mg/L, [PMS] = 0.4 mM, initial pH = 6.8, T = 30 °C.	100% with 30 min	SO <sub>4</sub> <sup>•−</sup>	[38]
Co <sub>3</sub> O <sub>4</sub> /C-BC/PMS	Bisphenol A (BPA)	[catalyst] = 0.3 g/L, [pollutant] = 20 mg/L, [PMS] = 1.0 mmol/L, [pH] = 7.0, [T] = 30 °C.	100% within less than 30 min	SO <sub>4</sub> <sup>•−</sup>	[39]
ZnO/biochar/PS	tetracycline hydrochloride (TC)	[TC] = 0.05 g/L, [ZnO200/BC] = 0.1 g/L, [PS] = 1.0 mM, pH = 7.0 ± 0.1, T = 25 ± 2 °C.	44.98% with 50 min	SO <sub>4</sub> <sup>•−</sup> and •OH	[40]
microwave irradiation(MW)/CuO/PS	2,4-dichlorophenol (2,4-DCP)	[PS] = 0.4 g/L, [CuO] = 40 mg/L, (2,4-DCP) = 50 mg/L, initial pH = 9, MW power intensity = 180 W.	>98% with 90 min	SO <sub>4</sub> <sup>•−</sup>	[41]
Ultrasound/Fe <sup>0</sup> /PS	Sulfadiazine (SD)	[SD] = 20 mg/L, [Fe <sup>0</sup> ] = 0.92 Mm, [PS] = 1.84 mM, US input power = 90 W, initial pH = 7, room temperature.	99.1% with 60 min	SO <sub>4</sub> <sup>•−</sup>	[42]
granular activated carbon (GAC)/PMS	Acid Orange 7 (AO7)	[AO7] = 20 mg/L, [PMS]: [AO7] = 100:1, [GAC] = 1.0 g/L, without pH adjustment, T = 20 ± 0.5 °C.	85% with 5 h	SO <sub>4</sub> <sup>•−</sup>	[43]
Fe <sub>3</sub> O <sub>4</sub> @Graphene oxide (GO)/PS	Rhodamine B (RhB)	[RhB] = 20 ppm, [Fe <sub>3</sub> O <sub>4</sub> @GO] = 500 mg/L, [PS] = 1.5 mM, pH = 4.34, T = 20 °C.	89% with 120 min	SO <sub>4</sub> <sup>•−</sup>	[44]
alkali and CuO/PS	Cu-ethylenediamine tetraacetic acid (Cu(II)-EDTA)	[Cu(II)-EDTA] = 3.14 mM, [PS]/[Cu(II)-EDTA] = 15:1, [CuO] = 2 g/L, pH maintained at 11.	Nearly 100% with 120 min	SO <sub>4</sub> <sup>•−</sup> , •OH and O <sub>2</sub> <sup>•−</sup>	[45]

### 3.1. Energy Activation

The activation process of PMS and PS through energy is shown in Figure 1. Energy input methods include heating, ultraviolet light, electricity, ultrasound, and radiation. It has been reported that at least 33.5 kcal/mol is required to break the O-O bond of  $S_2O_8^{2-}$  by heat [46]. Therefore, PS activation occurs only when the temperature reaches the required activation energy. Liang et al. found that PS could not be activated to achieve degradation of trichloroethylene and 1,1, 1-trichloroethane at 20 °C, whereas pollutants degradation could occur at 40–60 °C, and they found that the reaction with higher activation energy was more sensitive to temperature [47,48]. Yang et al. found that heating activation of PS is effective, but the activation efficiency of PMS is very low [49]. The combination of ultrasound and light with PS or PMS has received much attention in recent years as a potential alternative method for removal of refractory or toxic compounds. When  $H_2O_2$ , PS and PMS were activated by UV light, the removal rate of was 100% in the presence of PS and PMS, but only 75% in the presence of  $H_2O_2$  [50]. 1,1, 1-trichloroethane could be completely removed by ultrasonic activation of sodium persulfate, and the main ROS were  $SO_4^{\bullet-}$  and  $\bullet OH$  [23]. It has also been reported that laser can activate PS to produce  $SO_4^{\bullet-}$ , but there are few studies on its application in pollutant removal in recent years [51]. Although energy input can activate PMS and PS to produce free radicals, the generation efficiency of free radicals is generally low, accompanied by large energy output and high cost.



**Figure 1.** The activation reactions of PMS (a) and PS (b) by energy.

### 3.2. Transition Metal Ions Activation

In addition to energy activation, transition metal ions such as  $Co^{2+}$ ,  $Ce^{3+}$ ,  $Mn^{2+}$ ,  $Ni^{2+}$ , and  $Fe^{2+}$  can also activate PMS and PS. The reaction processes are redox reaction, as shown in Equations (1) and (2) [46]. There are many studies on the activation of PMS by  $Co^{2+}$ , and the relevant mechanism is basically clear, as shown in Figure 2. It mainly converts  $Co^{2+}$  into  $CoOH^+$ , then generates  $SO_4^{\bullet-}$  radical and  $CoO^+$ , further converts into  $Co^{3+}$ , and finally turns into  $Co^{2+}$  to complete the catalytic process [52]. The results show that  $Co^{2+}$  is the most efficient metal for activating PMS, while  $Ag^+$  is the most efficient metal for activating PS [30].  $Co^{2+}$ /PMS system is better than traditional Fenton oxidation, which can not only react under neutral conditions, but also has lower drug consumption [30].  $CoOH^+$  is the most effective intermediate substance in the reaction process of  $Co^{2+}$  activation of PMS, and its formation is the rate-limiting step of the reaction, as shown in Equation (3). The regeneration of  $Co^{2+}$  is realized through the reduction reaction of  $Co^{3+}$ , which is a key step to maintain the low usage of cobalt, as shown in Equation (4) [5].

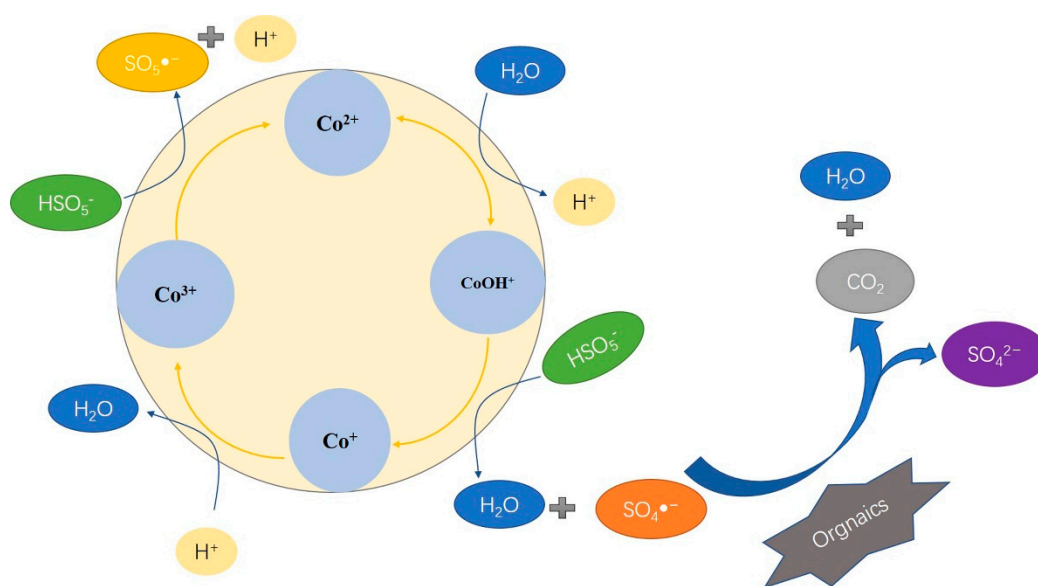
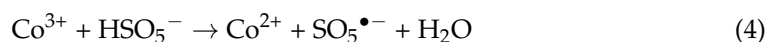
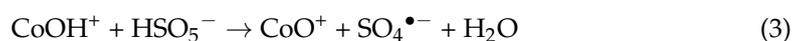
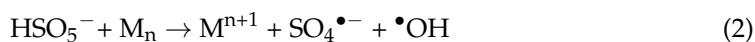
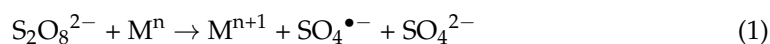


**Figure 2.** Mechanism diagram of Co catalyst activated PMS for degradation of organic pollutants.



Although cobalt ions have good activation ability of PMS, cobalt metals are toxic. The average concentration of cobalt in human serum and urine is about 0.1–0.3  $\mu\text{g}/\text{L}$  and 0.1  $\mu\text{g}/\text{L}$ , respectively [53]. Studies have shown that excessive cobalt may be potentially toxic and carcinogenic to human body, causing some diseases, such as asthma, pneumonia, and cardiomyopathy [5]. Therefore, the activation of PMS with cobalt-based materials has great environmental risks.  $\text{Ag}^+$  has better activation effect on PS, but silver is a precious metal, which is not easy to achieve large-scale application because of high cost. Iron-based materials have attracted widespread attention because of their non-toxic, large reserves and low price.  $\text{Fe}^{2+}$  can activate PMS and PS effectively, while  $\text{Fe}^{3+}$  has poor activation effect [54]. For homogeneous reaction systems, dissolved metal ions can react freely with PS and PMS, so mass transfer has little influence on the activation of PS and PMS. However, homogeneous reaction also has some disadvantages: (1) the dissolved metal ions are difficult to recover; (2) high concentration of organic wastewater will use a lot of metal salts, resulting in secondary pollution of metal ions in sewage; (3) transition metal ions are easily affected by water quality components and pH, such as precipitation under alkaline conditions, hydrolysis under acidic conditions, thus reducing the activation efficiency; and (4) in addition, some organic compounds in sewage will be complex with metal ions, which will also affect the activation of PS or PMS.

### 3.3. Transition Metal Oxide Activation

In order to overcome the problem of secondary contamination of homogeneous catalysts, researchers gradually shifted their research focus to heterogeneous catalytic reactions. Transition metal oxides also have good activation effect on persulfate. For example, five typical cobalt oxides ( $\text{CoO}$ ,  $\text{CoO}_2$ ,  $\text{Co}_2\text{O}_3$ ,  $\text{CoO}(\text{OH})$ , and  $\text{Co}_3\text{O}_4$ ) have been reported. Among them,  $\text{CoO}$  and  $\text{Co}_3\text{O}_4$  have been studied the most frequently, while  $\text{CoO}_2$  has thermal

instability and receives less attention. Dionysiou's group first studied the activation of PMS by CoO or Co<sub>3</sub>O<sub>4</sub>, and found that CoO/PMS systems tend to be homogeneous reactions because CoO has a high solubility in water (0.313 mg/100 g H<sub>2</sub>O) [7]. When Co<sub>3</sub>O<sub>4</sub> was used to activate PMS, the amount of cobalt dissolved was significantly reduced, mainly because CoO was inserted into the lattice of Co<sub>2</sub>O<sub>3</sub>, which made the structure relatively stable [55]. Co<sub>3</sub>O<sub>4</sub> has been widely studied for activating PMS due to its relatively high stability. In addition to the synthesis of Co<sub>3</sub>O<sub>4</sub> nanomaterials with various morphs, researchers also composite it with various carriers to prepare a variety of cobalt-supported materials to activate PMS. Carbon fiber, activated carbon, graphene, red mud, zeolite, SBA-15, and other materials are used as support materials [13]. Potential environmental risks and high cost limit the application of cobalt materials. In order to replace cobalt-based materials, other metal oxides such as MnO<sub>2</sub>, CuO, Fe<sub>3</sub>O<sub>4</sub>, Fe<sub>2</sub>O<sub>3</sub>, ZnO, and MFe<sub>2</sub>O<sub>4</sub> (M = Cu, Co, Mn, and Zn) have also been applied to PMS and PS activation studies, as shown in Figure 3. The mechanisms of PMS and PS activation by metal oxides are similar to that of homogeneous metal ions, which mainly depends on the redox action of metal ions [6]. According to the reduction mechanism, the activation of PS and PMS is positively correlated with the redox potential of the metal. In fact, metal redox potential is not the only factor affecting the activation of PS and PMS. For example, the redox potential of Ce<sup>3+</sup> is higher than that of Fe<sup>2+</sup>, but the activation effect is worse than that of Fe<sup>2+</sup> [56]. Therefore, the mechanism and process of metals activating PMS or PS still need to be further studied, and low-cost, efficient, and stable metal catalytic materials also need to be developed and applied.

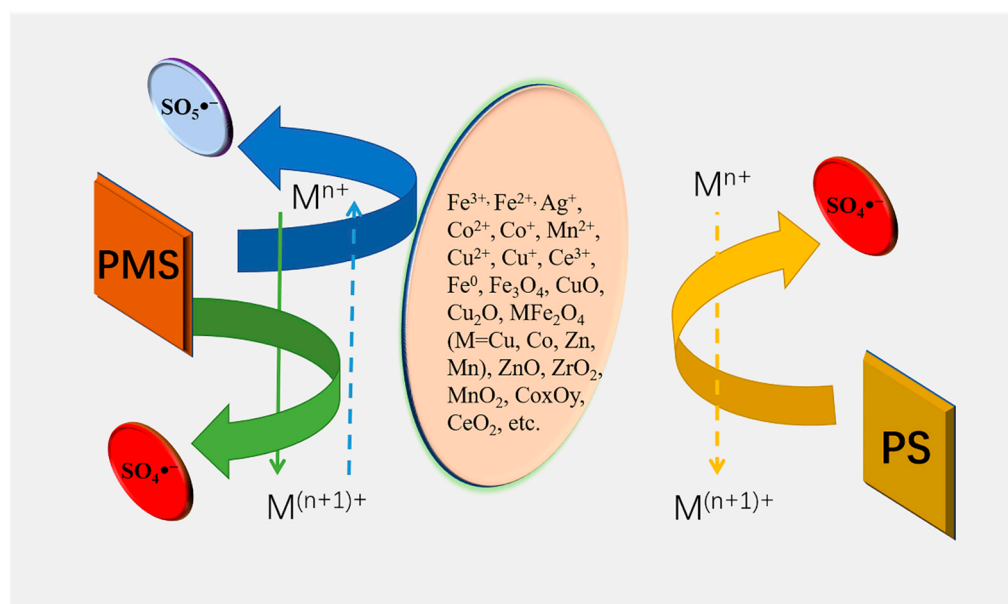
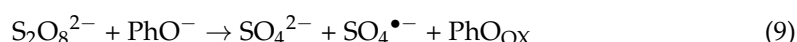
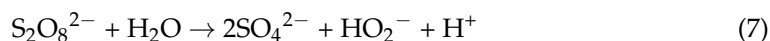
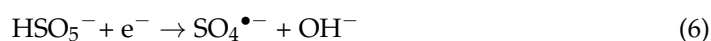
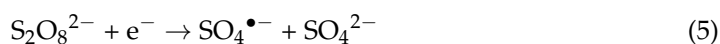


**Figure 3.** The mechanism diagram of PMS and PS activation by metal ions and metal oxides.

### 3.4. Non-Metallic Materials Activation

Recently, the most studied non-metallic catalytic materials are carbon-based materials, which have been widely used as adsorbent or carrier materials due to their large specific surface area, low cost, and large pore capacity. It was found that carbon-based materials can also activate PMS and PS well, and electron conduction is the main mechanism. It was found that carbon-based materials can also activate persulfate well, and electron conduction is the main mechanism. For example, the sp<sup>2</sup> covalent carbon net structure of multiwalled carbon nanotube forms a redox cycle with the oxygen-containing functional group at the edge defect, which provides electrons to activate PS to generate SO<sub>4</sub><sup>•−</sup> radicals [57]. In another form, electrons may be transferred from the carbon-based material of the aromatic graphite structure to PMS or PS [58]. PS and PMS are activated to produce SO<sub>4</sub><sup>•−</sup> radicals by receiving electrons, as shown in Equations (5) and (6). The structure and composi-

tion of carbon-based materials affect the redox potential and further affect the electron transfer reactions.



In addition, alkali, phenols, and quinones can also activate PS to generate  $\text{SO}_4^{\bullet-}$  radicals, as shown in Equations (7)–(9), while they activate PMS to generate singlet oxygen [6]. In order to improve the activation efficiency, the catalyst will be added at the same time with UV light, ultrasound and other energy input to promote the generation of free radicals.

Heterogeneous catalysis technology has the characteristics of high efficiency, low energy consumption, continuous catalysis, catalyst recovery, and less secondary pollution, which makes it become the mainstream research direction in many studies and shows a better application prospect. PMS and PS heterogeneous activation relies only on catalysts and oxidants, so the key lies in the development of low-cost, stable and efficient heterogeneous catalysts. Current reports mainly focus on the synthesis of laboratory-scale catalysts and the degradation of emerging pollutants. The pollutants treated are relatively single, and there is a lack of data for actual wastewater treatment. In addition, the preparation of catalytic materials reported is relatively complex, which is still a long way from large-scale production.

#### 4. Singlet Oxygen-Based Advanced Oxidation

With the report of PMS and PS non-radical activation, people gradually have a strong interest in the process of non-radical oxidation. Non-radical reactive species are generally thought to be resistant to common free radical scavengers (e.g., methanol, ethanol, and tert-butanol), selective to electron-rich organic compounds, and particularly sensitive to organic substrates with mild redox potentials [8]. At present, non-radical oxidation processes have been found in a variety of reaction systems, especially in PMS and PS activation. However, the mechanism remains controversial. Based on current reports, carbon or metal catalysts mainly realize non-radical activation of oxidants (PMS, PS,  $\text{H}_2\text{O}_2$ , or  $\text{O}_3$ ) through three ways: electron transfer process, generation of activated complexes (or surface-bound radicals) and singlet oxygen participating in pollutant degradation, respectively, as shown in Figure 4. Among them,  $^1\text{O}_2$  shows significant advantages in the selective removal of organic pollutants, which has become the focus of research.

##### 4.1. Properties of Singlet Oxygen

$^1\text{O}_2$  is an excited molecular oxygen, which is the excited state of the ground state oxygen (triplet oxygen molecule,  $^3\Sigma_g^-$ ). Originally, two electrons in two  $2p\pi^*$  orbitals with two spins parallel to each other can occupy one  $2p\pi^*$  orbital with opposite spins, or two  $2p\pi^*$  orbitals with opposite spins [59]. They're labeled as  $\text{O}_2(^1\Delta_g)$  and  $\text{O}_2(^1\Sigma_g^+)$ . Since  $\text{O}_2(^1\Sigma_g^+)$  has a short lifetime ( $10^{-12}$  s) and is easily converted to low-excited  $\text{O}_2(^1\Delta_g)$  ( $10^{-3}$ – $10^{-6}$  s), what is commonly called singlet oxygen is  $\text{O}_2(^1\Delta_g)$  [60].  $^1\text{O}_2$  is a non-radical substance with an energy of 94.2 kJ/mol, higher than the ground state oxygen molecule ( $\text{O}_2$ ). As a mildly oxidizing species, the standard redox potential ( $E_0 = 1.52$  V) of  $^1\text{O}_2$  was significantly lower than  $\bullet\text{OH}$  and  $\text{SO}_4^{\bullet-}$  [59]. Due to the vacant orbitals,  $^1\text{O}_2$  can obtain electrons from other substances and is a kind of electrophilic reagent

with mild reaction. Therefore, it can quickly oxidize organic pollutants with electron-rich functional groups and is not easy to be inactivated by background components in water [61]. Due to unique properties,  $^1\text{O}_2$  has been used for selective oxidation [62], degradation of organic pollutants [10], inactivation of pathogenic bacteria [63], cancer treatment [64], etc.  $^1\text{O}_2$  could be detected by chemical probe tests, electron paramagnetic resonance (EPR) spectroscopy and chemiluminescence detection.  $^1\text{O}_2$  could rapidly react with sodium azide ( $k = 1 \times 10^9 \text{ M}^{-1}\text{s}^{-1}$ ) and furfuryl alcohol ( $k = 1.2 \times 10^8 \text{ M}^{-1}\text{s}^{-1}$ ), but it is insensitive to alcohols (such as Et and TBA) [65]. Moreover,  $^1\text{O}_2$  can be detected by using 2,2,6,6-tetramethyl-4-piperidinol (TEMP) as a spin trapping agent in EPR with an intensive 1:1:1 signal [16]. In addition, solid-state near infrared spectroscopy and Fluorescence detection are helpful technique for  $^1\text{O}_2$  detection [64,66].

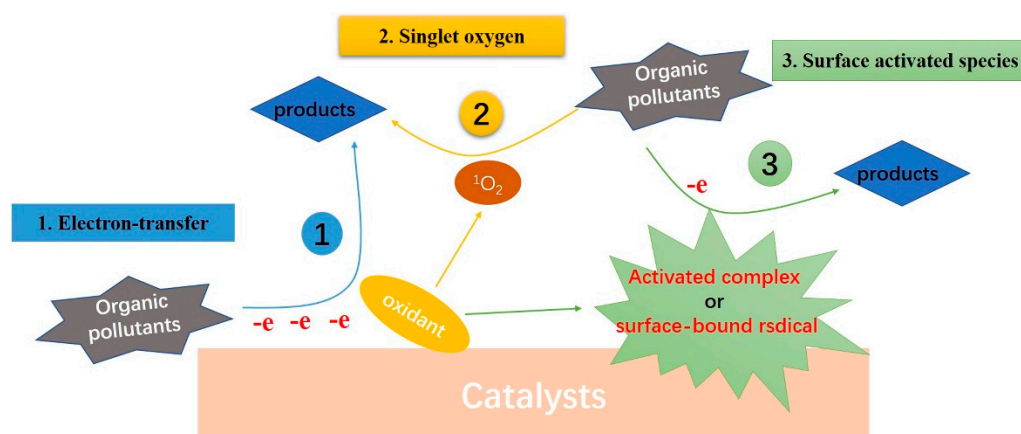


**Figure 4.** Schematic diagram of organic pollutants degradation by non-radical AOPs (Oxidant can be PMS, PS,  $\text{H}_2\text{O}_2$  or  $\text{O}_3$ ).

Previous reports have indicated that  $^1\text{O}_2$  can be produced by a photochemical process that uses photosensitization to transfer light energy to molecular oxygen [67]. For example, Dorota et al. successfully inactivated *Escherichia coli* and *Aspergillus fumigatus* using a miniature photoreactor to produce  $^1\text{O}_2$  [68]. In artificial or natural water, natural organic matter is used as photosensitizer to generate  $^1\text{O}_2$  through sunlight irradiation [69,70]. Other studies have shown that  $^1\text{O}_2$  can be generated by photoactivation of oxygen molecules in the oxidation of semiconductor metals such as  $\text{TiO}_2$  [71]. Studies on the generation of  $^1\text{O}_2$  by non-photosensitive methods are also emerging. It has been reported that catalysts such as  $\text{BiAg}_x\text{O}_y$  and  $\text{Bi(V)-Bi(III)}$  complex were used to release lattice oxygen to generate  $^1\text{O}_2$ , which could remove pollutants such as Rhodamine B and Bisphenol A [72,73]. Similarly,  $\text{MgO}$  with high-energy {111} crystal planes and  $\alpha\text{-Bi}_2\text{O}_3$  with oxygen vacancies can react with  $\text{O}_2$  to produce  $^1\text{O}_2$  [74]. In addition, phosphite reaction with ozone [75],  $\text{H}_2\text{O}_2$  reaction with  $\text{NaClO}$  [76], and the activation of periodate acid [77] can generate  $^1\text{O}_2$ . With the development of PMS and PS activation studies,  $^1\text{O}_2$  can also be generated by non-radical activation of PMS or PS, which provides a new path for the selective removal of organic pollutants. The relevant studies are summarized in Table 3.

**Table 3.** The removal of pollutants via  $^1\text{O}_2$  oxidation generated by PMS and PS activation.

Reaction System	Pollutant	Conditions	Reactivity	Dominant ROS	Ref.
Chlorophenols/PMS	2, 4, 6-trichlorophenol (2, 4, 6-TCP)	[2, 4, 6-TCP] = 25 $\mu\text{M}$ , [PMS] = 0.325 mM, T = $20 \pm 2$ $^\circ\text{C}$ , pH = 9.	95% with 60 min	$^1\text{O}_2$	[55]
benzoquinone (BQ)/PMS	sulfamethoxazole (SMX)	[PMS] = 0.44 mM, [SMX] = 8 $\mu\text{M}$ , [BQ] = 10 $\mu\text{M}$ , pH = 10, T = 25 $^\circ\text{C}$ .	86% with 3 min	$^1\text{O}_2$	[78]
PMS/base	Methylene blue (MB)	[PMS] = 1 mM, [MB] = 0.03 mM, [NaOH] = 2 mM, without pH adjustment	100% with 120 min	$^1\text{O}_2$	[79]
pyrophosphate (PA)/PMS	Acid Orange 7 (AO7)	[AO7] = 50 $\mu\text{M}$ , [PA] = 0.1 M, [PMS] = 2.5 mM, pH 9.5.	Nearly 100% with 10 min	$^1\text{O}_2$	[80]
Phosphite ( $\text{HPO}_3^{2-}$ )/PMS	Acid Orange 7 (AO7)	[AO7] = 20 mg/L, [PMS] = 10.0 mM, [ $\text{HPO}_3^{2-}$ ] = 25.0 mM, pH = 7.06.	82.1% within 60 min	$^1\text{O}_2$	[81]
$\text{NaBO}_2$ /PMS	Acid Red 1	[AR1] = 50 $\mu\text{M}$ , [PMS] = 3 mM, [ $\text{NaBO}_2$ ] = 7.5 mM, initial pH = 7.0, T = 30 $^\circ\text{C}$ .	97.8% within 10 min	$^1\text{O}_2$	[82]
carbonate ( $\text{CO}_3^{2-}$ )/PMS	Acid Orange 7 (AO7)	[AO7] = 0.05 mM, [ $\text{CO}_3^{2-}$ ] = 5 mM, [PMS] = 1 mM.	100% within 40 min	$\text{O}_2^-$ and $^1\text{O}_2$	[83]
$\beta\text{-MnO}_2$ /PS	phenol	[ $\beta\text{-MnO}_2$ ] = 400 mg/L, [PS] = 4 mM, [phenol] = 100 $\mu\text{M}$ , pH buffered around 6.5.	Over 99% with 180 min	$^1\text{O}_2$	[65]
$\text{CeVO}_4$ /PMS	phenol	Phenol = 100 ppm, $\text{CeVO}_4$ = 1.0 g/L, PMS = 2.0 g/L.	100% with 80 min	$^1\text{O}_2$	[84]
$\epsilon\text{-MnO}_2$ /PMS	Ciprofloxacin (CIP)	[CIP] = 10 ppm, [catalyst] = 0.1 g/L, [PMS] = 1 mM, without pH adjustment.	84.3% with 120 min	$^1\text{O}_2$	[85]
$\text{CuOMgO}/\text{Fe}_3\text{O}_4$ /PMPMS	4-chlorophenol (4-CP)	[4-CP] = 40 ppm, [PMS] = 2 mM, [catalyst] = 0.2 g/L, T = 30 $^\circ\text{C}$ .	100% within 40 min	$^1\text{O}_2$	[86]
$\text{CuO-CeO}_2$ /PMS	Rhodamine B (RhB)	[PMS] = 1.6 mM, [catalyst] = 0.4 g/L, initial pH 7, [RhB] = 0.1 mM.	100% within 60 min	$^1\text{O}_2$	[10]
$\text{CuO-Fe}_3\text{O}_4$ /PMS	Acid Orange 7 (AO7)	[ $\text{Na}_2\text{SO}_4$ ] = 0.2 M, [PMS] = 2 mM, [catalyst] = 0.1 g/L, initial pH = 7, [AO7] = 0.2 mM.	95.81% within 30 min	$^1\text{O}_2$	[87]
Iron centers on manganese oxides ( $\text{FeMn-350}$ )/PMS	bisphenol A (BPA)	[BPA] = 80 mg/L, [catalyst] = 0.5 g/L, [Oxone] = 0.6 mM, pH = 7.5.	Nearly 100% within 25 min	$^1\text{O}_2$	[88]
copper substituted zinc ferrite (ZCFO)/PMS	Ciprofloxacin (CIP)	[ZCFO] = 0.1 g/L, [PMS] = 2.5 mM, [CIP] = 10 mg/L and pH = 7.5.	96.6% with 15 min	$\text{O}_2^-$ and $^1\text{O}_2$	[89]
carbon nanotubes (CNTs)/PS	2,4-dichlorophenol (2,4-DCP)	[2,4-DCP] = 0.031 mM, PS/2,4-DCP molar ratio = 1/1, [CNTs] = 0.10 g/L, pH = $6.50 \pm 0.05$ .	95.9% within 30 min	$^1\text{O}_2$	[61]
Nanodiamonds (AND/800)/PMS	4-chlorophenol (4-CP)	[4-CP] = 0.16 mM, [PMS] = 0.25 mM, [AND/800] = 0.1 g/L, T = $20 \pm 2$ $^\circ\text{C}$ .	81% with 30 min	$^1\text{O}_2$	[90]
nitrogen-doped carbon nanosheets (NCN-900)/PMS	Bisphenol A (BPA)	[BPA] = 0.1 mM, [NCN-900] = 0.1 g/L, [PMS] = 2 mM, T = 30 $^\circ\text{C}$ , initial pH = 6.7.	100% within 2 min	$^1\text{O}_2$	[91]
N-doped porous carbon ( $\text{NC}_{1.0}$ )/PMS	Bisphenol A (BPA)	[BPA] = 0.1 mM, [ $\text{NC}_{1.0}$ ] = 0.2 g/L, [PMS] = 2 mM, T = 30 $^\circ\text{C}$ , initial pH = 6.7.	100% within 15 min	$^1\text{O}_2$	[92]
nitrogen-doped carbon nanotubes frameworks (NCNTFs)/PMS	Bisphenol A (BPA)	[BPA] = 25 mg/L, [NCNTFs-800] = 0.05 g/L, [Oxone] = 0.40 g/L, temperature = 20 $^\circ\text{C}$ .	97.3% with 30 min	$^1\text{O}_2$	[93]
$\text{CuO-Biochar}$ /PMS	Atrazine (ATZ)]	[ $\text{Na}_2\text{SO}_4$ ] = 200 mM, [PMS] = 2 mM, [catalyst] = 0.2 g/L, [ATZ] = 0.1 mM, initial pH = 7.	100% within 30 min	$^1\text{O}_2$	[94]
N-doped graphene/PMS	phenol	[catalyst] = 100 mg/L, [PMS] = 3.25 mM, [phenol] = 50 ppm, T = 25 $^\circ\text{C}$ .	100% within 30 min	$^1\text{O}_2$	[95]

#### 4.2. Homogeneous Activation

In recent years, it has been reported that  $^1\text{O}_2$  is produced by activated PMS via non-radical pathway leading to organic pollutants degradation. It has been found that ketones, phenols, quinones, and other hydrocarbons can activate PMS to produce  $^1\text{O}_2$ . Zhou et al. reported that benzoquinone can activate PMS to produce  $^1\text{O}_2$  through a non-free radical pathway, and found that the removal rate of sulfamethoxazole gradually increased with

the increase in solution pH from 7 to 10 [83]. As early as 1974, it was reported that ketones can activate PMS and that the decomposition rate of PMS is proportional to the amount of low concentration ketones [96]. Later, Lange and Brauer detected  $^1\text{O}_2$  at 1270 nm using infrared phosphorescence measurement technology, confirming the formation of  $^1\text{O}_2$  in the ketone-catalyzed PMS process [97]. Since phenolic compounds are easily oxidized to quinone as by-products, phenols can also activate PMS. Zhou et al. found that PMS was activated by phenol to generate  $^1\text{O}_2$  at pH 8.5 and 10, and phenol was oxidized to benzoquinone to further promote the activation reaction [55]. However, under acidic conditions, the dissociation of phenol is poor and it is difficult to form intramolecular complex with ionized PMS, resulting in difficult activation reaction

In fact, alkali has been used as a typical PS activator in site restoration, while it activates PMS to produce  $^1\text{O}_2$  [79]. PMS can spontaneously decompose to produce  $^1\text{O}_2$  under alkaline conditions, and the reaction rate constant is about  $0.2 \text{ M}^{-1}\text{s}^{-1}$  [78]. Moreover, polyphosphate [80], phosphite ( $\text{HPO}_3^{2-}$ ) [81],  $\text{BO}_2^-$  [82], and  $\text{CO}_3^{2-}$  [83] have also been found to activate PMS to produce  $^1\text{O}_2$  to degrade organic pollutants. All of the above are homogeneous reactions, activators are added into solution continuously to ensure continuity of the reaction, which is prone to high costs and secondary pollution. Therefore, heterogeneous activation reaction will be a good solution.

#### 4.3. Heterogeneous Activation

Metal oxides and complexes can also activate PMS and PS in a non-radical way. Bu et al. found that oxygen vacancy on bismuth bromide (BiOBr) could activate PS to produce  $^1\text{O}_2$  as the main active species to degrade Bisphenol A under alkaline conditions [98]. The sillenite  $\text{Bi}_{25}\text{FeO}_{40}$  was synthesized by hydrothermal method and used to activate PMS to degrade levofloxacin [99]. The results showed that  $^1\text{O}_2$  was the main ROS. Yang et al. synthesized  $\text{Fe}^0$ -montmorillonite composite material (Fe-Mt-C-H<sub>2</sub>) to activate PMS for the degradation of Bisphenol A [100]. It could remove 99.3% of Bisphenol A (25 mg/L) at pH 3 with 0.4 g/L Fe-Mt-C-H<sub>2</sub> and 1 mM PMS. The mineralization rate was 70.6%, and the degradation of pollutants was dominated by  $^1\text{O}_2$  and superoxide radical ( $\text{O}_2^{\bullet-}$ ). Liu et al. used  $\text{Co}_3\text{O}_4$ - $\text{SnO}_2$ /rice straw biochar (0.1 g/L) to activate PMS (1 mmol/L) to degrade sulfamoxole (50 mg/L), which was degraded 98% in 5 min by  $^1\text{O}_2$  [101].  $\text{CoOOH}$  [102] and  $\gamma$ - $\text{MnOOH}$  [103] were also used to activate PMS to degrade 2,4-dichlorophenol, which proved that  $^1\text{O}_2$  had a good removal effect on it. Li et al. used CuO-based modified materials to activate PMS to treat high-salt organic wastewater, and confirmed that the non-radical oxidation process led by  $^1\text{O}_2$  has a good removal effect on heterocyclic organic pollutants in a complex background [10,87,94]. Although the catalysis of PS or PMS by various metal oxides and their complexes has been studied endlessly, the environmental risks caused by metal ion leaching still exist in metal catalysts, and the separation and reuse of catalysts also face challenges.

A variety of carbon materials, including carbon nanotubes (CNTs), graphene oxide (GO), reduced graphene oxide (rGO), carbon spheres, nano-diamond and biochar, have been demonstrated to activate persulfate through a  $^1\text{O}_2$ -dominated non-radical pathway [104]. Cheng et al. used CNTs and PS combined system to efficiently generate  $^1\text{O}_2$  under no irradiation, which could selectively oxidize 2,4-dichlorophenol in water under neutral conditions [61]. CNTs not only act as electronic bridges between PS and organic pollutants, but also play an important role in the presence of various oxygen-containing functional groups (such as  $-\text{COOH}$ ,  $\text{C}=\text{O}$ , and  $-\text{OH}$ ) on the surface of CNTs, because they directly affect the zeta potential of CNTs, which is conducive to the absorption of PS, and promote the non-radical oxidation process of target pollutants [105]. GO and its reduced derivatives rGO show great potential in hydrophilic adsorption of organic matter and PMS/PS catalysis due to various structural defects, vacancies and oxygen-containing functional groups. Density Functional theory (DFT) calculations show that the vacancy and defect edges of rGO elongate the O-O bond of PMS, enhance adsorption and direct electron transfer, and promote the final rupture of the O-O bond, leading to non-radical oxida-

tion [106]. The increased degree of carbonyl and graphitization results in more vacancies and defects, thus improving the catalytic performance of GO and rGO [107]. N-doping is also an effective strategy. N-doped carbon is expected to have more lattice defects to regulate the electronic structure, such as  $sp^2$  hybrid carbon skeleton [108]. Doping nitrogen into the carbon matrix not only facilitates the adsorption of PMS, increases the surface alkalinity, but also facilitates the transfer of electrons to the negatively charged PMS, thus improving the catalytic activity. Biomass type and pyrolysis temperature are important factors affecting the structure and catalytic activity of biochar. Similarly, more oxygen vacancies, defects and oxygen-containing functional groups are still important factors in achieving  $^1O_2$  production from non-radical activated PMS and PS [109]. Carbon materials can not only achieve catalytic function, but also have the ability to adsorb pollutants, so it has great application potential. However, carbon materials have a variety of structural and surface characteristics, and the identification of their internal active sites is still difficult and controversial.

The studies on the degradation of organic pollutants by  $^1O_2$  have been reported, but there are still many problems to be solved, such as the preparation of high efficiency and stable catalysts, optimization of catalyst scale production process, clarifying the activation mechanism from different catalysts, explaining the interaction processes of  $^1O_2$  with organic pollutants, and effect of coexisting substances in wastewater on organic degradation process. In particular, few studies have been reported on the removal of organic pollutants in high-salt wastewater. The removal effect of organic pollutants in high-salt system, degradation kinetics, degradation intermediates and toxicity, the influence of inorganic salts type and concentration on the degradation process, and catalytic reaction mechanism remain to be solved.

## 5. Conclusions and Prospect

In this paper, the related research on  $SO_4^{\bullet-}$ -based and  $^1O_2$ -based AOPs has been reviewed, and the production methods and mechanism of  $SO_4^{\bullet-}$  and  $^1O_2$  are analyzed. Compared with the advanced oxidation process dominated by  $\bullet OH$ , the  $SO_4^{\bullet-}$ -based AOPs have a series of advantages such as long half-life of  $SO_4^{\bullet-}$ , wide range of pH application and strong oxidation capacity, which have a greater advantage in the removal of refractory pollutants. The non-radical oxidation process based on  $^1O_2$  has certain resistance to a variety of inorganic ions, halogens and background organic matter, strong selectivity and moderate redox potential, which can be used for the pre-oxidation treatment of highly dangerous industrial wastewater, pharmaceutical and pesticide wastewater. The  $SO_4^{\bullet-}$ -based and  $^1O_2$ -based AOPs have their own characteristics, which have good application prospects in the field of water purification and the removal of refractory organic pollutants from complex matrix. According to the existing research reports,  $SO_4^{\bullet-}$ -based and  $^1O_2$ -based AOPs still have some limitations.

(1) Most existing research has focused on treating single-component pollutants in the laboratory. However, actual wastewater is complex and variable. Although many research studies have been very successful on a laboratory scale, many problems need to be solved before large-scale practical applications. Especially, it should pay attention to addressing amplification issues such as design challenges, low energy requirements, and complex water quality changes. The next step is to study multi-component organic wastewater in real environment, and systematically study the reaction mechanisms by combining various characterization techniques and theoretical calculations, so as to further promote the popularization and application of this technology.

(2) There are still controversial including the mechanisms of PMS and PS activated by various catalysts. For example, the biochar-based materials will generate a variety of morphological structures and surface functional groups due to different raw materials and preparation methods. Therefore, the mechanisms of activating PMS and PS will be different. It is necessary to systematically study the relationship between material configuration and the efficiency of  $SO_4^{\bullet-}$  and  $^1O_2$  production. In addition, the catalysts should be prepared

from materials that are easily available and cheap, and the preparation process should be simple, energy saving, and easy to large-scale production.

(3) There are some unavoidable drawbacks for a single activation method. For example, thermal activation will lead to higher energy consumption, alkaline activation will affect the pH value of the system, electrochemical activation will produce more anode slime, carbon-based catalyst activation will make it difficult to regenerate, homogeneous transition metal activation will produce metal ions and sludge, resulting in secondary pollution, etc. The next step is to overcome the shortcomings of each activation method and maximize the development of multiple combined activation methods.

(4) Considering that  $^1\text{O}_2$  has strong anti-interference ability to inorganic salts and natural organics, while  $\text{SO}_4^{\bullet-}$  and  $\bullet\text{OH}$  have strong oxidation ability, the reaction system can be designed according to the treated objects to achieve phased and multi-channel activation of PS and PMS. It is expected to achieve higher oxidation efficiency by selectively regulating the production of strong oxidizing radicals ( $\text{SO}_4^{\bullet-}$  and  $\bullet\text{OH}$ ) and non-radical ( $^1\text{O}_2$ ) according to water quality and pollutant types and concentration levels, which will provide ideas for the practical application of this technology.

(5) In addition to the removal of refractory pollutants,  $^1\text{O}_2$  as a non-radical ROS can be used to inactivate pathogenic microorganisms and remove antibiotic resistance genes in natural water and drinking water. Obviously, there are few studies and reports on this aspect. Although  $\text{SO}_4^{\bullet-}$  has strong oxidation ability, it costs a lot to treat high-concentration organic wastewater. Hence, it is necessary to combine  $\text{SO}_4^{\bullet-}$ -based AOPs with traditional biological and physicochemical treatment to achieve the lowest operating cost. It is urgent to carry out research works in this field.

(6) The effectiveness of AOPs depends to a large extent on the generation rate of ROS and the contact with pollutant molecules. It should be paid to the reduction in oxidant dosage and the efficient recycling of catalysts. There are significantly fewer studies based on PS activation than on PMS activation, and new technologies for PS activation are still limited. In fact, commercial PS is much cheaper than PMS, and PS activation produces fewer  $\text{SO}_4^{2-}$  ions than PMS activation because PMS only makes up a third of Oxone. Therefore, more attention should be paid to the activation research of PS, especially the research and development of related catalysts and activation methods is very important for the future commercial application.

**Author Contributions:** Conceptualization, Z.L. and M.Y.; methodology, D.L.; software, Y.S.; validation, F.C., H.L. and Y.D.; formal analysis, Z.L.; investigation, Y.S.; resources, M.Y.; data curation, D.L.; writing—original draft preparation, Z.L.; writing—review and editing, Y.S.; visualization, M.Y.; supervision, D.L.; project administration, F.C.; funding acquisition, M.Y. All authors have read and agreed to the published version of the manuscript.

**Funding:** This research was funded by [the National Nonprofit Institute Research Grants of TIWTE], grant number [TKS20220201, TKS20220204] and [research project of Shanghai Science and Technology Commission], grant number [19DZ1204303]. And The APC was funded by [the National Nonprofit Institute Research Grants of TIWTE].

**Conflicts of Interest:** The authors declare no conflict of interest.

## References

1. Wang, J.; Tian, Z.; Huo, Y.B.; Yang, M.; Zheng, X.C.; Zhang, Y. Monitoring of 943 organic micropollutants in wastewater from municipal wastewater treatment plants with secondary and advanced treatment processes. *J. Environ. Sci.* **2018**, *67*, 309–317. [[CrossRef](#)]
2. Tröger, R.; Klöckner, P.; Ahrens, L.; Wiberg, K. Micropollutants in drinking water from source to tap—Method development and application of a multiresidue screening method. *Sci. Total Environ.* **2018**, *627*, 1404–1432. [[CrossRef](#)]
3. Oh, W.-D.; Dong, Z.; Lim, T.-T. Generation of sulfate radical through heterogeneous catalysis for organic contaminants removal: Current development, challenges and prospects. *Appl. Catal. B Environ.* **2016**, *194*, 169–201. [[CrossRef](#)]
4. Xiao, G.; Xu, T.; Faheem, M.; Xi, Y.; Zhou, T.; Moryani, H.; Bao, J.; Du, J. Evolution of Singlet Oxygen by Activating Peroxydisulfate and Peroxymonosulfate: A Review. *Int. J. Environ. Res. Public Health* **2021**, *18*, 3344. [[CrossRef](#)]

5. Hu, P.; Long, M. Cobalt-catalyzed sulfate radical-based advanced oxidation: A review on heterogeneous catalysts and applications. *Appl. Catal. B Environ.* **2016**, *181*, 103–117. [[CrossRef](#)]
6. Ahmed, M.M.; Barbati, S.; Doumenq, P.; Chiron, S. Sulfate radical anion oxidation of diclofenac and sulfamethoxazole for water decontamination. *Chem. Eng. J.* **2012**, *197*, 440–447. [[CrossRef](#)]
7. Anipsitakis, G.P.; Dionysiou, D.D. Degradation of Organic Contaminants in Water with Sulfate Radicals Generated by the Conjunction of Peroxymonosulfate with Cobalt. *Environ. Sci. Technol.* **2003**, *37*, 4790–4797. [[CrossRef](#)]
8. Duan, X.; Sun, H.; Shao, Z.; Wang, S. Nonradical reactions in environmental remediation processes: Uncertainty and challenges. *Appl. Catal. B Environ.* **2018**, *224*, 973–982. [[CrossRef](#)]
9. Bokare, A.D.; Choi, W. Singlet-Oxygen Generation in Alkaline Periodate Solution. *Environ. Sci. Technol.* **2015**, *49*, 14392–14400. [[CrossRef](#)]
10. Li, Z.; Liu, D.; Zhao, Y.; Li, S.; Wei, X.; Meng, F.; Huang, W.; Lei, Z. Singlet oxygen dominated peroxymonosulfate activation by CuO-CeO<sub>2</sub> for organic pollutants degradation: Performance and mechanism. *Chemosphere* **2019**, *233*, 549–558. [[CrossRef](#)]
11. Mirza-Aghayan, M.; Tavana, M.M.; Boukherroub, R. Direct oxidative synthesis of nitrones from aldehydes and primary anilines using graphite oxide and Oxone. *Tetrahedron Lett.* **2014**, *55*, 5471–5474. [[CrossRef](#)]
12. Anipsitakis, G.P.; Tufano, T.P.; Dionysiou, D.D. Chemical and microbial decontamination of pool water using activated potassium peroxymonosulfate. *Water Res.* **2008**, *42*, 2899–2910. [[CrossRef](#)]
13. Ghanbari, F.; Moradi, M. Application of peroxymonosulfate and its activation methods for degradation of environmental organic pollutants: Review. *Chem. Eng. J.* **2017**, *310*, 41–62. [[CrossRef](#)]
14. House, D.A. Kinetics and Mechanism of Oxidations by Peroxydisulfate. *Chem. Rev.* **1962**, *62*, 185–203. [[CrossRef](#)]
15. Tang, L.; Ma, X.Y.; Wang, Y.; Zhang, S.; Zheng, K.; Wang, X.C.; Lin, Y. Removal of trace organic pollutants (pharmaceuticals and pesticides) and reduction of biological effects from secondary effluent by typical granular activated carbon. *Sci. Total Environ.* **2020**, *749*, 141611. [[CrossRef](#)]
16. Bu, Z.; Hou, M.; Li, Z.; Dong, Z.; Zeng, L.; Zhang, P.; Wu, G.; Li, X.; Zhang, Y.; Pan, Y. Fe<sup>3+</sup>/Fe<sup>2+</sup> cycle promoted peroxymonosulfate activation with addition of boron for sulfamethazine degradation: Efficiency and the role of boron. *Sep. Purif. Technol.* **2022**, *298*, 121596. [[CrossRef](#)]
17. Ding, Y.; Zhu, L.; Wang, N.; Tang, H. Sulfate radicals induced degradation of tetrabromobisphenol A with nanoscaled magnetic CuFe<sub>2</sub>O<sub>4</sub> as a heterogeneous catalyst of peroxymonosulfate. *Appl. Catal. B Environ.* **2012**, *129*, 153–162. [[CrossRef](#)]
18. Guan, Y.-H.; Ma, J.; Li, X.-C.; Fang, J.-Y.; Chen, L.-W. Influence of pH on the Formation of Sulfate and Hydroxyl Radicals in the UV/Peroxymonosulfate System. *Environ. Sci. Technol.* **2011**, *45*, 9308–9314. [[CrossRef](#)]
19. Acero, J.L.; Benítez, F.J.; Real, F.J.; Rodríguez, E. Degradation of selected emerging contaminants by UV-activated persulfate: Kinetics and influence of matrix constituents. *Sep. Purif. Technol.* **2018**, *201*, 41–50. [[CrossRef](#)]
20. Dong, Z.-Y.; Xu, B.; Hu, C.-Y.; Zhang, T.-Y.; Tang, Y.-L.; Pan, Y.; El-Din, M.G.; Xian, Q.-M.; Gao, N.-Y. The application of UV-C laser in persulfate activation for micropollutant removal: Case study with iodinated X-ray contrast medias. *Sci. Total Environ.* **2021**, *779*, 146340. [[CrossRef](#)]
21. Ghauch, A.; Tuqan, A.M.; Kibbi, N. Ibuprofen removal by heated persulfate in aqueous solution: A kinetics study. *Chem. Eng. J.* **2012**, *197*, 483–492. [[CrossRef](#)]
22. Ren, T.-L.; Ma, X.-W.; Wu, X.-Q.; Yuan, L.; Lai, Y.-L.; Tong, Z.-H. Degradation of imidazolium ionic liquids in a thermally activated persulfate system. *Chem. Eng. J.* **2021**, *412*, 128624. [[CrossRef](#)]
23. Li, B.; Li, L.; Lin, K.; Zhang, W.; Lu, S.; Luo, Q. Removal of 1,1,1-trichloroethane from aqueous solution by a sono-activated persulfate process. *Ultrason. Sonochem.* **2013**, *20*, 855–863. [[CrossRef](#)]
24. Frontistis, Z.; Mantzavinos, D.; Meriç, S. Degradation of antibiotic ampicillin on boron-doped diamond anode using the combined electrochemical oxidation—Sodium persulfate process. *J. Environ. Manag.* **2018**, *223*, 878–887. [[CrossRef](#)] [[PubMed](#)]
25. Ayoub, G.; Ghauch, A. Assessment of bimetallic and trimetallic iron-based systems for persulfate activation: Application to sulfamethoxazole degradation. *Chem. Eng. J.* **2014**, *256*, 280–292. [[CrossRef](#)]
26. Wang, S.; Wu, J.; Lu, X.; Xu, W.; Gong, Q.; Ding, J.; Dan, B.; Xie, P. Removal of acetaminophen in the Fe<sup>2+</sup>/persulfate system: Kinetic model and degradation pathways. *Chem. Eng. J.* **2018**, *358*, 1091–1100. [[CrossRef](#)]
27. Rastogi, A.; Al-Abed, S.R.; Dionysiou, D.D. Sulfate radical-based ferrous–peroxymonosulfate oxidative system for PCBs degradation in aqueous and sediment systems. *Appl. Catal. B Environ.* **2009**, *85*, 171–179. [[CrossRef](#)]
28. Hafeez, M.A.; Hong, S.J.; Jeon, J.; Lee, J.; Singh, B.K.; Hyatt, N.C.; Walling, S.A.; Heo, J.; Um, W. Co<sup>2+</sup>/PMS based sulfate-radical treatment for effective mineralization of spent ion exchange resin. *Chemosphere* **2022**, *287*, 132351. [[CrossRef](#)]
29. Nfodzo, P.; Choi, H. Triclosan decomposition by sulfate radicals: Effects of oxidant and metal doses. *Chem. Eng. J.* **2011**, *174*, 629–634. [[CrossRef](#)]
30. Anipsitakis, G.P.; Dionysiou, D.D. Radical Generation by the Interaction of Transition Metals with Common Oxidants. *Environ. Sci. Technol.* **2004**, *38*, 3705–3712. [[CrossRef](#)]
31. Peng, J.; Zhou, H.; Liu, W.; Ao, Z.; Ji, H.; Liu, Y.; Su, S.; Yao, G.; Lai, B. Insights into heterogeneous catalytic activation of peroxymonosulfate by natural chalcopyrite: pH-dependent radical generation, degradation pathway and mechanism. *Chem. Eng. J.* **2020**, *397*, 125387. [[CrossRef](#)]
32. Gao, Y.; Han, Y.; Liu, B.; Gou, J.; Feng, D.; Cheng, X. CoFe<sub>2</sub>O<sub>4</sub> nanoparticles anchored on waste eggshell for catalytic oxidation of florfenicol via activating peroxymonosulfate. *Chin. Chem. Lett.* **2022**, *33*, 3713–3720. [[CrossRef](#)]

33. Shen, Y.; de Vidales, M.J.M.; Gorni, G.; Gómez-Herrero, A.; Fernández-Martínez, F.; Dos Santos-García, A.J. Enhanced performance and recyclability for peroxymonosulfate activation via g-C<sub>3</sub>N<sub>4</sub> supported CoFe layer double oxide. *Chem. Eng. J.* **2022**, *444*, 136610. [[CrossRef](#)]
34. Chen, X.; Chen, J.; Qiao, X.; Wang, D.; Cai, X. Performance of nano-Co<sub>3</sub>O<sub>4</sub>/peroxymonosulfate system: Kinetics and mechanism study using Acid Orange 7 as a model compound. *Appl. Catal. B Environ.* **2008**, *80*, 116–121. [[CrossRef](#)]
35. Qi, F.; Chu, W.; Xu, B. Catalytic degradation of caffeine in aqueous solutions by cobalt-MCM41 activation of peroxymonosulfate. *Appl. Catal. B Environ.* **2013**, *134–135*, 324–332. [[CrossRef](#)]
36. Ouyang, M.; Li, X.; Xu, Q.; Tao, Z.; Yao, F.; Huang, X.; Wu, Y.; Wang, D.; Yang, Q.; Chen, Z.; et al. Heterogeneous activation of persulfate by Ag doped BiFeO<sub>3</sub> composites for tetracycline degradation. *J. Colloid Interface Sci.* **2020**, *566*, 33–45. [[CrossRef](#)]
37. Deng, J.; Ye, C.; Cai, A.; Huai, L.; Zhou, S.; Dong, F.; Li, X.; Ma, X. S-doping α-Fe<sub>2</sub>O<sub>3</sub> induced efficient electron-hole separation for enhanced persulfate activation toward carbamazepine oxidation: Experimental and DFT study. *Chem. Eng. J.* **2021**, *420*, 129863. [[CrossRef](#)]
38. Wu, Z.; Wang, Y.; Xiong, Z.; Ao, Z.; Pu, S.; Yao, G.; Lai, B. Core-shell magnetic Fe<sub>3</sub>O<sub>4</sub>@Zn/Co-ZIFs to activate peroxymonosulfate for highly efficient degradation of carbamazepine. *Appl. Catal. B Environ.* **2020**, *277*, 119136. [[CrossRef](#)]
39. Chen, X.-L.; Li, F.; Zhang, M.; Liu, B.; Chen, H.; Wang, H. Highly dispersed and stabilized Co<sub>3</sub>O<sub>4</sub>/C anchored on porous biochar for bisphenol A degradation by sulfate radical advanced oxidation process. *Sci. Total Environ.* **2021**, *777*, 145794. [[CrossRef](#)]
40. Xu, R.; Li, M.; Zhang, Q. Collaborative optimization for the performance of ZnO/biochar composites on persulfate activation through plant enrichment-pyrolysis method. *Chem. Eng. J.* **2021**, *429*, 132294. [[CrossRef](#)]
41. Ghorbanian, Z.; Asgari, G.; Samadi, M.T.; Seid-Mohammadi, A. Removal of 2,4 dichlorophenol using microwave assisted nanoscale zero-valent copper activated persulfate from aqueous solutions: Mineralization, kinetics, and degradation pathways. *J. Mol. Liq.* **2019**, *296*, 111873. [[CrossRef](#)]
42. Zou, X.; Zhou, T.; Mao, J.; Wu, X. Synergistic degradation of antibiotic sulfadiazine in a heterogeneous ultrasound-enhanced Fe<sup>0</sup>/persulfate Fenton-like system. *Chem. Eng. J.* **2014**, *257*, 36–44. [[CrossRef](#)]
43. Zhang, J.; Shao, X.; Shi, C.; Yang, S. Decolorization of Acid Orange 7 with peroxymonosulfate oxidation catalyzed by granular activated carbon. *Chem. Eng. J.* **2013**, *232*, 259–265. [[CrossRef](#)]
44. Pervez, N.; He, W.; Zarra, T.; Naddeo, V.; Zhao, Y. New Sustainable Approach for the Production of Fe<sub>3</sub>O<sub>4</sub>/Graphene Oxide-Activated Persulfate System for Dye Removal in Real Wastewater. *Water* **2020**, *12*, 733. [[CrossRef](#)]
45. Hong, Y.; Luo, Z.; Zhang, N.; Qu, L.; Zheng, M.; Suara, M.A.; Chelme-Ayala, P.; Zhou, X.; El-Din, M.G. Decomplexation of Cu(II)-EDTA by synergistic activation of persulfate with alkali and CuO: Kinetics and activation mechanism. *Sci. Total Environ.* **2022**, *817*, 152793. [[CrossRef](#)] [[PubMed](#)]
46. Zhang, B.-T.; Zhang, Y.; Teng, Y.; Fan, M. Sulfate Radical and Its Application in Decontamination Technologies. *Crit. Rev. Environ. Sci. Technol.* **2014**, *45*, 1756–1800. [[CrossRef](#)]
47. Liang, C.; Bruell, C.J. Thermally Activated Persulfate Oxidation of Trichloroethylene: Experimental Investigation of Reaction Orders. *Ind. Eng. Chem. Res.* **2008**, *47*, 2912–2918. [[CrossRef](#)]
48. Liang, C.J.; Bruell, C.J.; Marley, M.C.; Sperry, K.L. Thermally Activated Persulfate Oxidation of Trichloroethylene (TCE) and 1,1,1-Trichloroethane (TCA) in Aqueous Systems and Soil Slurries. *Soil Sediment Contam. Int. J.* **2003**, *12*, 207–228. [[CrossRef](#)]
49. Yang, S.; Wang, P.; Yang, X.; Shan, L.; Zhang, W.; Shao, X.; Niu, R. Degradation efficiencies of azo dye Acid Orange 7 by the interaction of heat, UV and anions with common oxidants: Persulfate, peroxymonosulfate and hydrogen peroxide. *J. Hazard. Mater.* **2010**, *179*, 552–558. [[CrossRef](#)]
50. He, X.; de la Cruz, A.A.; Dionysiou, D.D. Destruction of cyanobacterial toxin cylindrospermopsin by hydroxyl radicals and sulfate radicals using UV-254nm activation of hydrogen peroxide, persulfate and peroxymonosulfate. *J. Photochem. Photobiol. A Chem.* **2013**, *251*, 160–166. [[CrossRef](#)]
51. George, C.; Chovelon, J.-M. A laser flash photolysis study of the decay of SO<sub>4</sub><sup>-</sup> and Cl<sub>2</sub><sup>-</sup> radical anions in the presence of Cl<sup>-</sup> in aqueous solutions. *Chemosphere* **2002**, *47*, 385–393. [[CrossRef](#)]
52. Chen, X.; Qiao, X.; Wang, D.; Lin, J.; Chen, J. Kinetics of oxidative decolorization and mineralization of Acid Orange 7 by dark and photoassisted Co<sup>2+</sup>-catalyzed peroxymonosulfate system. *Chemosphere* **2006**, *67*, 802–808. [[CrossRef](#)] [[PubMed](#)]
53. Barceloux, D.G. Cobalt. *J. Toxicol. Clin. Toxicol.* **1999**, *37*, 201–216. [[CrossRef](#)]
54. Rodriguez, S.; Vasquez, L.; Costa, D.; Romero, A.; Santos, A. Oxidation of Orange G by persulfate activated by Fe(II), Fe(III) and zero valent iron (ZVI). *Chemosphere* **2014**, *101*, 86–92. [[CrossRef](#)]
55. Li, C.-X.; Wang, Y.-J.; Chen, C.-B.; Fu, X.-Z.; Cui, S.; Lu, J.-Y.; Liu, H.-Q.; Li, W.-W. Interactions between chlorophenols and peroxymonosulfate: pH dependency and reaction pathways. *Sci. Total Environ.* **2019**, *664*, 133–139. [[CrossRef](#)] [[PubMed](#)]
56. Wang, J.; Wang, S. Activation of persulfate (PS) and peroxymonosulfate (PMS) and application for the degradation of emerging contaminants. *Chem. Eng. J.* **2018**, *334*, 1502–1517. [[CrossRef](#)]
57. Duan, X.; Sun, H.; Kang, J.; Wang, Y.; Indrawirawan, S.; Wang, S. Insights into Heterogeneous Catalysis of Persulfate Activation on Dimensional-Structured Nanocarbons. *ACS Catal.* **2015**, *5*, 4629–4636. [[CrossRef](#)]
58. Jans, U.; Hoigné, J. Activated Carbon and Carbon Black Catalyzed Transformation of Aqueous Ozone into OH-Radicals. *Ozone: Sci. Eng.* **1998**, *20*, 67–90. [[CrossRef](#)]
59. Zhou, Y.; Jiang, J.; Gao, Y.; Pang, S.-Y.; Yang, Y.; Ma, J.; Gu, J.; Li, J.; Wang, Z.; Wang, L.-H.; et al. Activation of peroxymonosulfate by phenols: Important role of quinone intermediates and involvement of singlet oxygen. *Water Res.* **2017**, *125*, 209–218. [[CrossRef](#)]

60. Schweitzer, C.; Schmidt, R. Physical Mechanisms of Generation and Deactivation of Singlet Oxygen. *Chem. Rev.* **2003**, *103*, 1685–1758. [[CrossRef](#)]
61. Cheng, X.; Guo, H.; Zhang, Y.; Wu, X.; Liu, Y. Non-photochemical production of singlet oxygen via activation of persulfate by carbon nanotubes. *Water Res.* **2017**, *113*, 80–88. [[CrossRef](#)] [[PubMed](#)]
62. Krieger-Liszakay, A. Singlet oxygen production in photosynthesis. *J. Exp. Bot.* **2005**, *56*, 337–346. [[CrossRef](#)] [[PubMed](#)]
63. Hotze, E.M.; Badireddy, A.R.; Chellam, S.; Wiesner, M.R. Mechanisms of Bacteriophage Inactivation via Singlet Oxygen Generation in UV Illuminated Fullerol Suspensions. *Environ. Sci. Technol.* **2009**, *43*, 6639–6645. [[CrossRef](#)] [[PubMed](#)]
64. Yuan, Y.; Zhang, C.-J.; Xu, S.; Liu, B. A self-reporting AIE probe with a built-in singlet oxygen sensor for targeted photodynamic ablation of cancer cells. *Chem. Sci.* **2015**, *7*, 1862–1866. [[CrossRef](#)]
65. Zhu, S.; Li, X.; Kang, J.; Duan, X.; Wang, S. Persulfate Activation on Crystallographic Manganese Oxides: Mechanism of Singlet Oxygen Evolution for Nonradical Selective Degradation of Aqueous Contaminants. *Environ. Sci. Technol.* **2018**, *53*, 307–315. [[CrossRef](#)]
66. Rkanofsky, J. Assay for singlet-oxygen generation by peroxidases using 1270-nm chemiluminescence. *Methods Enzymol.* **2000**, *319*, 59–67.
67. Qu, X.; Alvarez, P.J.J.; Li, Q. Photochemical Transformation of Carboxylated Multiwalled Carbon Nanotubes: Role of Reactive Oxygen Species. *Environ. Sci. Technol.* **2013**, *47*, 14080–14088. [[CrossRef](#)]
68. Bartusik, D.; Aebisher, D.; Lyons, A.M.; Greer, A. Bacterial Inactivation by a Singlet Oxygen Bubbler: Identifying Factors Controlling the Toxicity of  $^1\text{O}_2$  Bubbles. *Environ. Sci. Technol.* **2012**, *46*, 12098–12104. [[CrossRef](#)]
69. Romero, O.C.; Straub, A.P.; Kohn, T.; Nguyen, T.H. Role of Temperature and Suwannee River Natural Organic Matter on Inactivation Kinetics of Rotavirus and Bacteriophage MS2 by Solar Irradiation. *Environ. Sci. Technol.* **2011**, *45*, 10385–10393. [[CrossRef](#)]
70. Mostafa, S.; Rosario-Ortiz, F.L. Singlet Oxygen Formation from Wastewater Organic Matter. *Environ. Sci. Technol.* **2013**, *47*, 8179–8186. [[CrossRef](#)]
71. Guo, X.; Li, Q.; Zhang, M.; Long, M.; Kong, L.; Zhou, Q.; Shao, H.; Hu, W.; Wei, T. Enhanced photocatalytic performance of N-nitrosodimethylamine on  $\text{TiO}_2$  nanotube based on the role of singlet oxygen. *Chemosphere* **2015**, *120*, 521–526. [[CrossRef](#)] [[PubMed](#)]
72. Zhang, T.; Ding, Y.; Tang, H. Generation of singlet oxygen over Bi(V)/Bi(III) composite and its use for oxidative degradation of organic pollutants. *Chem. Eng. J.* **2015**, *264*, 681–689. [[CrossRef](#)]
73. Yu, K.; Yang, S.; Boyd, S.A.; Chen, H.; Sun, C. Efficient degradation of organic dyes by BiAgxOy. *J. Hazard. Mater.* **2011**, *197*, 88–96. [[CrossRef](#)] [[PubMed](#)]
74. Hao, Y.-J.; Liu, B.; Tian, L.-G.; Li, F.-T.; Ren, J.; Liu, S.-J.; Liu, Y.; Zhao, J.; Wang, X.-J. Synthesis of {111} Facet-Exposed MgO with Surface Oxygen Vacancies for Reactive Oxygen Species Generation in the Dark. *ACS Appl. Mater. Interfaces* **2017**, *9*, 12687–12693. [[CrossRef](#)]
75. Stephenson, L.M.; McClure, D.E. Mechanisms in phosphite ozonide decomposition to phosphate esters and singlet oxygen. *J. Am. Chem. Soc.* **1973**, *95*, 3074–3076. [[CrossRef](#)]
76. Foote, C.S.; Wexler, S.; Ando, W.; Higgins, R. Chemistry of singlet oxygen. IV. Oxygenations with hypochlorite-hydrogen peroxide. *J. Am. Chem. Soc.* **1968**, *90*, 975–981. [[CrossRef](#)]
77. Du, J.; Xiao, G.; Xi, Y.; Zhu, X.; Su, F.; Kim, S.H. Periodate activation with manganese oxides for sulfanilamide degradation. *Water Res.* **2020**, *169*, 115278. [[CrossRef](#)]
78. Zhou, Y.; Jiang, J.; Gao, Y.; Ma, J.; Pang, S.-Y.; Li, J.; Lu, X.-T.; Yuan, L.-P. Activation of Peroxymonosulfate by Benzoquinone: A Novel Nonradical Oxidation Process. *Environ. Sci. Technol.* **2015**, *49*, 12941–12950. [[CrossRef](#)]
79. Yang, F.; Huang, Y.; Fang, C.; Xue, Y.; Ai, L.; Liu, J.; Wang, Z. Peroxymonosulfate/base process in saline wastewater treatment: The fight between alkalinity and chloride ions. *Chemosphere* **2018**, *199*, 84–88. [[CrossRef](#)]
80. Lou, X.; Fang, C.; Geng, Z.; Jin, Y.; Xiao, D.; Wang, Z.; Liu, J.; Guo, Y. Significantly enhanced base activation of peroxymonosulfate by polyphosphates: Kinetics and mechanism. *Chemosphere* **2017**, *173*, 529–534. [[CrossRef](#)]
81. Peng, G.; You, W.; Zhou, W.; Zhou, G.; Qi, C.; Hu, Y. Activation of peroxymonosulfate by phosphite: Kinetics and mechanism for the removal of organic pollutants. *Chemosphere* **2020**, *266*, 129016. [[CrossRef](#)] [[PubMed](#)]
82. Rao, L.; Yang, Y.; Chen, L.; Liu, X.; Chen, H.; Yao, Y.; Wang, W. Highly efficient removal of organic pollutants via a green catalytic oxidation system based on sodium metaborate and peroxymonosulfate. *Chemosphere* **2019**, *238*, 124687. [[CrossRef](#)] [[PubMed](#)]
83. Nie, M.; Zhang, W.; Yan, C.; Xu, W.; Wu, L.; Ye, Y.; Hu, Y.; Dong, W. Enhanced removal of organic contaminants in water by the combination of peroxymonosulfate and carbonate. *Sci. Total Environ.* **2018**, *647*, 734–743. [[CrossRef](#)] [[PubMed](#)]
84. Othman, I.; Zain, J.H.; Abu Haija, M.; Banat, F. Catalytic activation of peroxymonosulfate using  $\text{CeVO}_4$  for phenol degradation: An insight into the reaction pathway. *Appl. Catal. B Environ.* **2020**, *266*, 118601. [[CrossRef](#)]
85. Chi, Y.; Wang, P.; Lin, M.; Lin, C.; Gao, M.; Zhao, C.; Wu, X. Manganese oxides activated peroxymonosulfate for ciprofloxacin removal: Effect of oxygen vacancies and chemical states. *Chemosphere* **2022**, *299*, 134437. [[CrossRef](#)]
86. Jawad, A.; Zhan, K.; Wang, H.; Shahzad, A.; Zeng, Z.; Wang, J.; Zhou, X.; Ullah, H.; Chen, Z.; Chen, Z. Tuning of Persulfate Activation from a Free Radical to a Nonradical Pathway through the Incorporation of Non-Redox Magnesium Oxide. *Environ. Sci. Technol.* **2020**, *54*, 2476–2488. [[CrossRef](#)]

87. Li, Z.; Sun, Y.; Huang, W.; Xue, C.; Zhu, Y.; Wang, Q.; Liu, D. Innovatively employing magnetic CuO nanosheet to activate peroxymonosulfate for the treatment of high-salinity organic wastewater. *J. Environ. Sci.* **2020**, *88*, 46–58. [[CrossRef](#)]
88. Yu, L.; Zhang, G.; Liu, C.; Lan, H.; Liu, H.; Qu, J. Interface Stabilization of Undercoordinated Iron Centers on Manganese Oxides for Nature-Inspired Peroxide Activation. *ACS Catal.* **2018**, *8*, 1090–1096. [[CrossRef](#)]
89. Yu, R.; Zhao, J.; Zhao, Z.; Cui, F. Copper substituted zinc ferrite with abundant oxygen vacancies for enhanced ciprofloxacin degradation via peroxymonosulfate activation. *J. Hazard. Mater.* **2019**, *390*, 121998. [[CrossRef](#)]
90. Shao, P.; Tian, J.; Yang, F.; Duan, X.; Gao, S.; Shi, W.; Luo, X.; Cui, F.; Luo, S.; Wang, S. Identification and Regulation of Active Sites on Nanodiamonds: Establishing a Highly Efficient Catalytic System for Oxidation of Organic Contaminants. *Adv. Funct. Mater.* **2018**, *28*, 1705295. [[CrossRef](#)]
91. Gao, Y.; Chen, Z.; Zhu, Y.; Li, T.; Hu, C. New Insights into the Generation of Singlet Oxygen in the Metal-Free Peroxymonosulfate Activation Process: Important Role of Electron-Deficient Carbon Atoms. *Environ. Sci. Technol.* **2019**, *54*, 1232–1241. [[CrossRef](#)] [[PubMed](#)]
92. Gao, Y.; Li, T.; Zhu, Y.; Chen, Z.; Liang, J.; Zeng, Q.; Lyu, L.; Hu, C. Highly nitrogen-doped porous carbon transformed from graphitic carbon nitride for efficient metal-free catalysis. *J. Hazard. Mater.* **2019**, *393*, 121280. [[CrossRef](#)] [[PubMed](#)]
93. Ma, W.; Wang, N.; Fan, Y.; Tong, T.; Han, X.; Du, Y. Non-radical-dominated catalytic degradation of bisphenol A by ZIF-67 derived nitrogen-doped carbon nanotubes frameworks in the presence of peroxymonosulfate. *Chem. Eng. J.* **2018**, *336*, 721–731. [[CrossRef](#)]
94. Li, Z.; Liu, D.; Huang, W.; Wei, X.; Huang, W. Biochar supported CuO composites used as an efficient peroxymonosulfate activator for highly saline organic wastewater treatment. *Sci. Total Environ.* **2020**, *721*, 137764. [[CrossRef](#)]
95. Liang, P.; Zhang, C.; Duan, X.; Sun, H.; Liu, S.; Tade, M.O.; Wang, S. An insight into metal organic framework derived N-doped graphene for the oxidative degradation of persistent contaminants: Formation mechanism and generation of singlet oxygen from peroxymonosulfate. *Environ. Sci. Nano* **2017**, *4*, 315–324. [[CrossRef](#)]
96. Montgomery, R.E. Catalysis of peroxymonosulfate reactions by ketones. *J. Am. Chem. Soc.* **1974**, *96*, 7820–7821. [[CrossRef](#)]
97. Lange, A.; Brauer, H.-D. On the formation of dioxiranes and of singlet oxygen by the ketone-catalysed decomposition of Caro's acid. *J. Chem. Soc. Perkin Trans. 2* **1996**, *5*, 805–811. [[CrossRef](#)]
98. Bu, Y.; Li, H.; Yu, W.; Pan, Y.; Li, L.; Wang, Y.; Pu, L.; Ding, J.; Gao, G.; Pan, B. Peroxydisulfate Activation and Singlet Oxygen Generation by Oxygen Vacancy for Degradation of Contaminants. *Environ. Sci. Technol.* **2021**, *55*, 2110–2120. [[CrossRef](#)]
99. Liu, Y.; Guo, H.; Zhang, Y.; Tang, W.; Cheng, X.; Li, W. Heterogeneous activation of peroxymonosulfate by sillenite Bi<sub>25</sub>FeO<sub>40</sub>: Singlet oxygen generation and degradation for aquatic levofloxacin. *Chem. Eng. J.* **2018**, *343*, 128–137. [[CrossRef](#)]
100. Yang, S.; Wu, P.; Liu, J.; Chen, M.; Ahmed, Z.; Zhu, N. Efficient removal of bisphenol A by superoxide radical and singlet oxygen generated from peroxymonosulfate activated with Fe<sup>0</sup>-montmorillonite. *Chem. Eng. J.* **2018**, *350*, 484–495. [[CrossRef](#)]
101. Liu, L.; Li, Y.; Li, W.; Zhong, R.; Lan, Y.; Guo, J. The efficient degradation of sulfisoxazole by singlet oxygen (<sup>1</sup>O<sub>2</sub>) derived from activated peroxymonosulfate (PMS) with Co<sub>3</sub>O<sub>4</sub>-SnO<sub>2</sub>/RSBC. *Environ. Res.* **2020**, *187*, 109665. [[CrossRef](#)] [[PubMed](#)]
102. Zhang, Q. Mechanism and Performance of Singlet Oxygen Dominated Peroxymonosulfate Activation on CoOOH Nanoparticles for 2,4-Dichlorophenol Degradation in Water. *J. Hazard. Mater.* **2020**, *8*.
103. He, D.; Li, Y.; Lyu, C.; Song, L.; Feng, W.; Zhang, S. New insights into MnOOH/peroxymonosulfate system for catalytic oxidation of 2,4-dichlorophenol: Morphology dependence and mechanisms. *Chemosphere* **2020**, *255*, 126961. [[CrossRef](#)] [[PubMed](#)]
104. Yu, J.; Feng, H.; Tang, L.; Pang, Y.; Zeng, G.; Lu, Y.; Dong, H.; Wang, J.; Liu, Y.; Feng, C.; et al. Metal-free carbon materials for persulfate-based advanced oxidation process: Microstructure, property and tailoring. *Prog. Mater. Sci.* **2020**, *111*, 100654. [[CrossRef](#)]
105. Ren, W.; Xiong, L.; Nie, G.; Zhang, H.; Duan, X.; Wang, S. Insights into the Electron-Transfer Regime of Peroxydisulfate Activation on Carbon Nanotubes: The Role of Oxygen Functional Groups. *Environ. Sci. Technol.* **2019**, *54*, 1267–1275. [[CrossRef](#)]
106. Duan, X.; Ao, Z.; Zhou, L.; Sun, H.; Wang, G.; Wang, S. Occurrence of radical and nonradical pathways from carbocatalysts for aqueous and nonaqueous catalytic oxidation. *Appl. Catal. B Environ.* **2016**, *188*, 98–105. [[CrossRef](#)]
107. Chen, X.; Oh, W.-D.; Lim, T.-T. Graphene- and CNTs-based carbocatalysts in persulfates activation: Material design and catalytic mechanisms. *Chem. Eng. J.* **2018**, *354*, 941–976. [[CrossRef](#)]
108. Gao, Y.; Zhu, Y.; Lyu, L.; Zeng, Q.; Xing, X.; Hu, C. Electronic Structure Modulation of Graphitic Carbon Nitride by Oxygen Doping for Enhanced Catalytic Degradation of Organic Pollutants through Peroxymonosulfate Activation. *Environ. Sci. Technol.* **2018**, *52*, 14371–14380. [[CrossRef](#)]
109. Huang, B.-C.; Jiang, J.; Huang, G.-X.; Yu, H.-Q. Sludge biochar-based catalysts for improved pollutant degradation by activating peroxymonosulfate. *J. Mater. Chem. A* **2018**, *6*, 8978–8985. [[CrossRef](#)]